AGU PUBLICATIONS

Geochemistry, Geophysics, Geosystems

RESEARCH ARTICLE
10.1002/2017GC007073

**Key Points:**
- Field-induced anisotropy between <2% and 270% of initial AMS, and can influence AMS shape, degree, or principal directions
- Increase of susceptibility parallel to last applied AF orientation may lead to switching of principal axes
- Problematic if AMS is carried by ferromagnetic minerals, and degree of anisotropy is low

**Supporting Information:**
- Supporting Information S1
- Figure S1
- Figure S2
- Table S1

**Correspondence to:**
A. R. Biedermann,
andrea.regina.biedermann@gmail.com

**Citation:**
Biedermann, A. R., M. Jackson, D. Bilardello, J. M. Feinberg, M. C. Brown, and S. A. McEnroe (2017), Influence of static alternating field demagnetization on anisotropy of magnetic susceptibility: Experiments and implications, *Geochem. Geophys. Geosyst.*, *18*, doi:10.1002/2017GC007073.

Received 19 JUN 2017
Accepted 10 AUG 2017
Accepted article online 12 AUG 2017



# Influence of static alternating field demagnetization on anisotropy of magnetic susceptibility: Experiments and implications

**Andrea R. Biedermann[1], Mike Jackson[1], Dario Bilardello[1], Joshua M. Feinberg[1], Maxwell C. Brown[2], and Suzanne A. McEnroe[3]**

[1]Institute for Rock Magnetism, University of Minnesota, Minneapolis, Minnesota, USA, [2]Institute of Earth Sciences, University of Iceland, Reykjavík, Iceland, [3]Department of Geoscience and Petroleum, Norwegian University of Science and Technology, Trondheim, Norway

**Abstract** Anisotropy of magnetic susceptibility (AMS) indicates the preferred orientation of a rock's constituent minerals. However, other factors can influence the AMS, e.g., domain wall pinning or domain alignment in ferromagnetic minerals. Therefore, it is controversial whether samples should be alternating field (AF) demagnetized prior to AMS characterization. This may remove the influence of natural remanent magnetization (NRM) or domain wall pinning on AMS; however, it may also result in field-induced anisotropy. This study investigates the influence of stepwise AF and low-temperature demagnetization on mean susceptibility, principal susceptibility directions, AMS degree and shape for sedimentary, metamorphic, and igneous rocks. Alternating fields up to 200 mT were applied along the sample *x*, *y*, and *z* axes, rotating the order for each step, to characterize the relationship between AMS principal directions and the last AF orientation. The changes in anisotropy, defined by the mean deviatoric susceptibility of the difference tensors, are between <2% and 270% of the AMS in NRM-state. Variations in AMS parameters range from small changes in shape to complete reorientation of principal susceptibility axes, with the maximum susceptibility becoming parallel to the last AF direction. This is most prevalent in samples with low degrees of anisotropy in the NRM-state. No clear correlations were found between field-induced anisotropy and hysteresis properties. Therefore, we propose that future studies check any samples whose AMS is carried by ferromagnetic minerals and low anisotropy degrees for AF-induced artifacts. These results highlight the need for understanding the AMS sources and carriers prior to any structural interpretation.

## 1. Introduction

The anisotropy of magnetic susceptibility (AMS) in a rock results mainly from the preferred alignment of its constituent minerals, and is therefore often used as a proxy for mineral fabric [*Borradaile and Jackson*, 2010; *Borradaile and Henry*, 1997; *Hrouda*, 1982; *Martín-Hernández et al*., 2004; *Tarling and Hrouda*, 1993]. It has been shown that if the AMS is dominantly carried by magnetite it can be directly related to the shape preferred orientation (SPO) of magnetite grains [*Archanjo et al*., 1995; *Archanjo et al*., 2002; *Grégoire et al*., 1995; *Grégoire et al*., 1998]. Similarly, if AMS is controlled by phyllosilicates, it reflects the phyllosilicate crystallographic preferred orientation (CPO) [*Chadima et al*., 2004; *Hirt et al*., 1995; *Lüneburg et al*., 1999; *Richter et al*., 1993; *Siegesmund et al*., 1995]. Recent studies have been successful in modeling whole-rock AMS from CPO data when several paramagnetic and diamagnetic minerals contribute, and in quantifying the contributions from each mineral [*Biedermann et al*., 2015c; *Martín-Hernandez et al*., 2005; *Schmidt et al*., 2009].

However, AMS can additionally be affected by other factors such as domain alignment during laboratory treatment, stress/magnetostriction or pressure, which are not reflected in the grain CPO or SPO [*Bhathal and Stacey*, 1969; *Jackson et al*., 1993; *Nishioka et al*., 2007; *Park et al*., 1988; *Potter and Stephenson*, 1990]. For example, *Park et al*. [1988] used (tumbling) AF treatment as a cleaning technique to remove an unstable component of the AMS that was unrelated to the SPO of magnetite, but related to later tectonic stress. The influence of domain alignment, also termed field-induced anisotropy or field-impressed anisotropy, was first described by *Stacey* [1961, 1963], who suggested that a small AMS is produced if multidomain (MD) particles are subjected to an alternating field (AF). *Bhathal and Stacey* [1969] stated that a rock's intrinsic AMS is

enhanced when applying an AF field parallel to its easy axis. A similar observation was made by *Violat and Daly* [1971] who found that the susceptibility parallel to the AF axis increased. These authors additionally reported that the directions of the principal susceptibility axes changed during AF treatment, and suggested that a field-imposed AMS, due to domain alignment in MD magnetite, could be superposed on the structural AMS. The same conclusion was reached by *Kapicka* [1981], who report that this effect is largest in rocks with higher coercivity, and absent in low-coercivity samples. On the contrary, an isotropic sample of single-domain (SD) $\gamma$-$Fe_2O_3$ has been observed to acquire an oblate AMS with the unique axis parallel to the applied field, thus decreasing the susceptibility parallel to the AF field [*Potter and Stephenson*, 1988]. This effect increased with stronger AF fields. These observations suggest that grain size strongly affects the size and shape of the impressed ellipsoid, with MD grains producing prolate ellipsoids, i.e., an increase in susceptibility parallel to the field axis, and SD grains oblate ellipsoids, i.e., a decrease in susceptibility in the direction of the field [*Potter and Stephenson*, 1990; *Stephenson et al*., 1995]. For the same reason, increases and decreases in susceptibility parallel to the last AF direction have been described for samples exhibiting normal (MD grains) or inverse magnetic fabrics (SD grains) [*Schöbel and de Wall*, 2014; *Schöbel et al*., 2013]. *Jordanova et al*. [2007] reported that the effect of AF field on susceptibility and AMS depends on the amount and size of large MD magnetite. Additionally, *Henry et al*. [2007] found a stronger AF-effect on mean susceptibility in samples with a higher degree of anisotropy.

*Halgedahl and Fuller* [1981, 1983] imaged domain wall patterns in pyrrhotite and Ti-magnetite, and observed a complicated pattern of undulating walls after thermal demagnetization, and a simple pattern of field-parallel 180° domain walls after AF demagnetization. They interpreted the AF treatment to unblock domain walls from their pinning sites. Whereas a model has been developed to quantify domain rearrangement in MD particles, some discrepancies remain [*Stephenson and Potter*, 1996].

Some studies have found that AF treatment enhances the AMS [*Bhathal and Stacey*, 1969; *Liu et al*., 2005]. Others have used AF cleaning to remove any secondary stress-related components from the AMS measurement [*Park et al*., 1988], or to avoid biases due to strong remanent magnetization [*Lanci*, 2010; *Schöbel and de Wall*, 2014; *Schöbel et al*., 2013]. While yet others treat field-induced anisotropy as an artefact [*Bhathal and Stacey*, 1969; *Henry et al*., 2007; *Jordanova et al*., 2007; *Potter and Stephenson*, 1990; *Violat and Daly*, 1971]. In line with these different interpretations, contradicting recommendations have been put forward as to whether or not samples should be AF demagnetized prior to AMS measurements: either (1) AMS should be measured before AF treatment, in order to avoid effects of artificial field-induced anisotropy [*Jordanova et al*., 2007; *Potter and Stephenson*, 1990] or (2) samples should be demagnetized before the AMS is determined, to remove the effects of stress-induced domain wall pinning, or to remove the effects of a strong natural remanent magnetization (NRM) [*Lanci*, 2010; *Liu et al*., 2005; *Park et al*., 1988; *Schöbel and de Wall*, 2014; *Schöbel et al*., 2013].

This study investigates how the susceptibility tensor changes from a rock's NRM state through progressive three-axis AF demagnetization up to 200 mT, during which the order of the AF axes are changed after each step. Additionally, these tensors are compared to those after low-temperature demagnetization. The primary goal of this contribution is not to explain the physical origin of field-induced anisotropy, but to characterize how it may affect magnetic fabric studies. The results shown here will help to estimate the effect of field-induced or stress-related contributions to anisotropy for a range of natural lithologies, and determine the optimal order of experiments for future studies.

## 2. Methods

### 2.1. Samples

A variety of samples has been used for this study, in order to investigate the influence of AF treatment on AMS for a number of different mineralogies and grain sizes. The sample collection includes (1) metamorphic rocks (n = 8 specimens) from the Thomson Slate, Minnesota, USA, whose AMS is carried by paramagnetic minerals and magnetite or Ti-magnetite [*Johns et al*., 1992; *Sun et al*., 1995], (2) sedimentary red beds (n = 6) of the Mauch Chunk Formation, Pennsylvania, containing magnetite and hematite [*Bilardello and Kodama*, 2010; *Tan and Kodama*, 2002], (3) igneous rocks (n = 7) from the cumulate series of the Bjerkreim Sokndal Layered Intrusion, Southern Norway, comprising MD and PSD magnetite and hemo-ilmenite [*Biedermann et al*., 2016b; *McEnroe et al*., 2001, 2009; *Robinson et al*., 2001], and (4) basalts (n = 14) from Fogo, Cape

Verde, containing a variety of grain sizes and domain states from MD to interacting SD magnetite, with compositions ranging from low-Ti titanomagnetite to high-Ti titanomagnetite (TM0 – TM70) [*Brown et al*., 2010].

### 2.2. Hysteresis Properties

Hysteresis loops and backfield curves were measured on a Princeton Measurements Corporation MicroMag Vibrating Sample Magnetometer, in order to define saturation magnetization (Ms) and remanence magnetization (Mr), as well as coercivity (Bc) and remanence coercivity (Bcr). These measurements were performed on one or several chips from the same samples on which the AMS and AF measurements were made, e.g., the tops and bottoms of drill cores.

### 2.3. AF Demagnetization

All samples were progressively demagnetized using a DTech D-2000 Precision Instruments AF demagnetizer, using field steps of 2, 5, 10, 15, 20, 30, 40, 50, 60, 70, 80, (90 for Thomson Slate, Mauch Chunk, Bjerkreim Sokndal, but not Fogo basalt samples) 100, 120, 140, 160, 180, and 200 mT. Slower AF decay rates were used for weak fields, and faster rates for stronger fields. No systematic changes of AMS properties were observed related to the changes in decay rate. AF demagnetization was performed along three perpendicular axes, with a cyclic permutation of the order of the axes (*x, y, z* or *y, z, x* or *z, x, y*) for successive steps. NRM and remaining magnetization after each AF step were measured on a 2G Enterprises 760-R (Mtn. View, CA, USA) RF SQUID superconducting rock magnetometer (SRM) housed inside a magnetically shielded room with a background field $<$300 nT. At high AF fields ($>$100 mT), the coils inside our DTech Precision Instruments AF (de)magnetizer heat up, and measurements of sample temperatures immediately after these demagnetization steps showed a maximum temperature increase of 10 K. Sample temperatures were measured using an optical thermometer, for two Mauch Chunk and six Thomson Slate samples before and after demagnetization for each step above 70 mT.

### 2.4. Low-Temperature Demagnetization

Subsequent to AF demagnetization, samples were demagnetized at low-temperature by cooling them in liquid nitrogen, and letting them warm up in a zero-field, inside a mu-metal shield within the shielded room (background field less than $\sim$20 nT). As it cools through its isotropic point and the Verwey transition, most of the remanent magnetization of MD magnetite is removed by this procedure [*Dunlop*, 2003; *Merrill*, 1970; *Morris et al*., 2009; *Muxworthy and McClelland*, 2000; *Ozima et al*., 1964]. Because both the remanence and field-induced anisotropy in MD magnetite are related to the organization of magnetic moments in domains, the rationale for employing this procedure was to remove any field-induced anisotropy due to domain wall alignment. In addition, whereas AF demagnetization may introduce an anisotropy because the field is applied in a set of antiparallel directions, the low-temperature demagnetization is an isotropic process which should not introduce any preferred directions.

### 2.5. AMS Measurements

AMS was measured in the NRM state and after each demagnetization step on an AGICO MFK1-FA susceptibility bridge operated at the instruments' standard field of 200 A/m and frequency of 976 Hz. The full susceptibility tensor was determined based on either 15 directional measurements, or measurements on a spinning sample in three perpendicular planes [*Jelinek*, 1977, 1996]. The results obtained with these two approaches are indistinguishable. The eigenvalues ($k_1 >= k_2 >= k_3$) and eigenvectors (defined by $D_1$ and $I_1$, $D_2$ and $I_2$, $D_3$ and $I_3$, where $D$ is declination and $I$ inclination) of the susceptibility tensor represent the principal susceptibilities and their directions. The mean susceptibility is defined as $k_{mean} = (k_1 + k_2 + k_3)/3$, and the degree and shape of anisotropy will be described by $P = k_1/k_3$ and $U = (2k_2 - k_1 - k_3)/(k_1 - k_3)$ [*Jelinek*, 1981; *Nagata*, 1961]. Higher values of $P$ indicate more extreme anisotropy, while positive (negative) values of $U$ indicate oblate (prolate) shaped tensors.

In addition to determining the full tensor after each demagnetization step, difference tensors were calculated (tensor after AF treatment minus tensor in NRM state) in order to quantify the effects of the field-induced anisotropy. Analogously, the difference tensor between the AMS in NRM state and AMS in low-temperature-demagnetized state serves to assess the effect of NRM on the AMS.

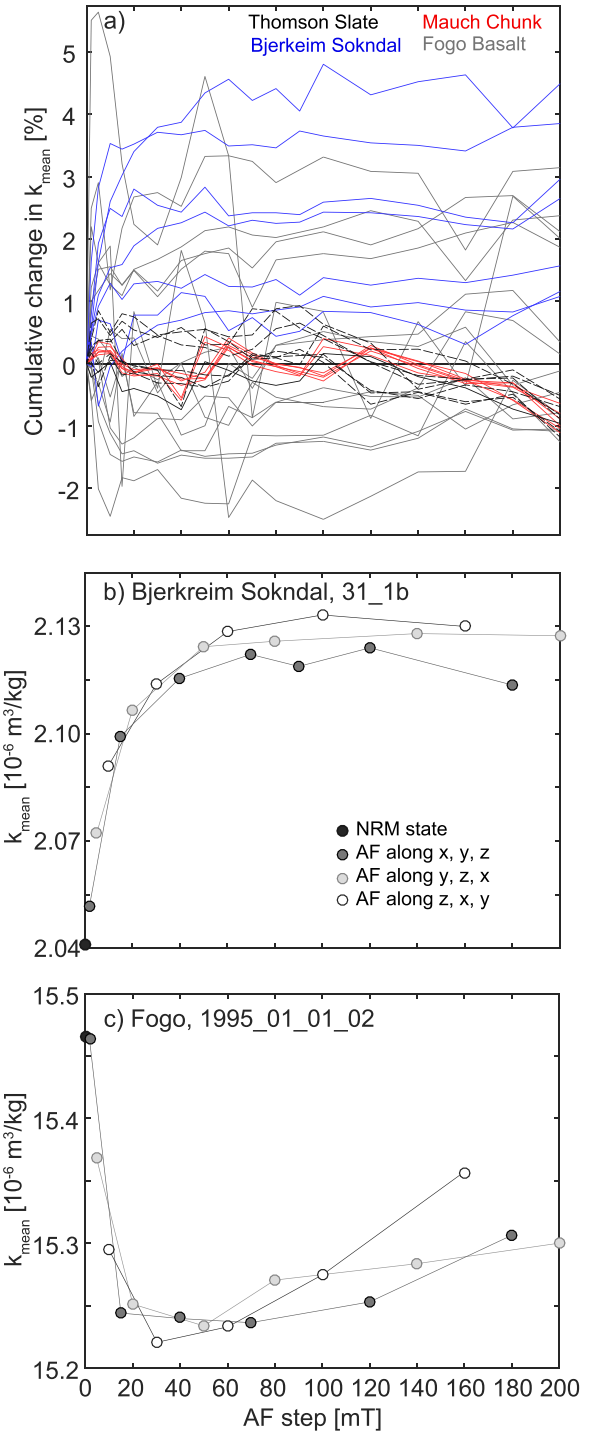


**Figure 1.** Effect of AF field, and orientation of last AF axis on the mean susceptibility.

## 3. Results

### 3.1. Changes in Mean Susceptibility

Two observations have been made regarding the influence of AF fields on mean susceptibility. In general, the variations in mean susceptibility compared to the NRM state are between −2% and +5% (Figure 1a), with the largest positive changes displayed by igneous samples from Bjerkreim Sokndal and some Fogo basalts in low AF fields (<20–50 mT). Another group of Fogo samples shows an initial decrease of mean susceptibility in fields <20 mT. Thomson Slate and Mauch Chunk samples show little variation in $k_{mean}$ initially, followed by a 1% decrease in fields >100 mT. In some samples, these general trends are accompanied by a small variation depending on the direction of the last applied field (Figures 1b and 1c).

After low temperature demagnetization, the mean susceptibility changes between −2.3% and +4.5% as compared to the $k_{mean}$ in NRM state. For Thomson Slate samples, the susceptibility generally decreases, and changes are between −0.5% and +0.1%. The susceptibility in Mauch Chunk red beds increases 0.6 to 0.8%. Larger increases of up to 4.5% are observed in igneous samples from Bjerkreim Sokndal, and the changes in Fogo basalt are −2.3% to +2.8%.

### 3.2. Changes in AMS During AF Treatment

Figure 2a shows a comparison between *P* and *U* in NRM state and during AF demagnetization, and Figures 2b–2e the change in *P* and *U* during treatment with increasing AF fields for samples representative of each group. For Thomson slates, the variation in P and U during demagnetization is small compared to the variation between sites, and the measurements for each sample are still separated from those of other samples. For the Fogo basalt samples, on the other hand, changes invoked by AF treatment are larger than the variation between samples.

No systematic variation of *P* and *U* with AF orientation can be seen in samples from the Thomson Slate. Red bed samples from the Mauch Chunk formation exhibit constant *P*, however, the AMS shape *U* changes systematically with increasing AF field and the order of the AF axes. The most pronounced effect is observed in the igneous rocks from Fogo and Bjerkreim Sokndal, which display changes in both *P* and *U* during AF treatment. Just as observed in the *U*-parameter of the Mauch Chunk samples, there is a strong dependence on the order of directions in which the AF field was applied.

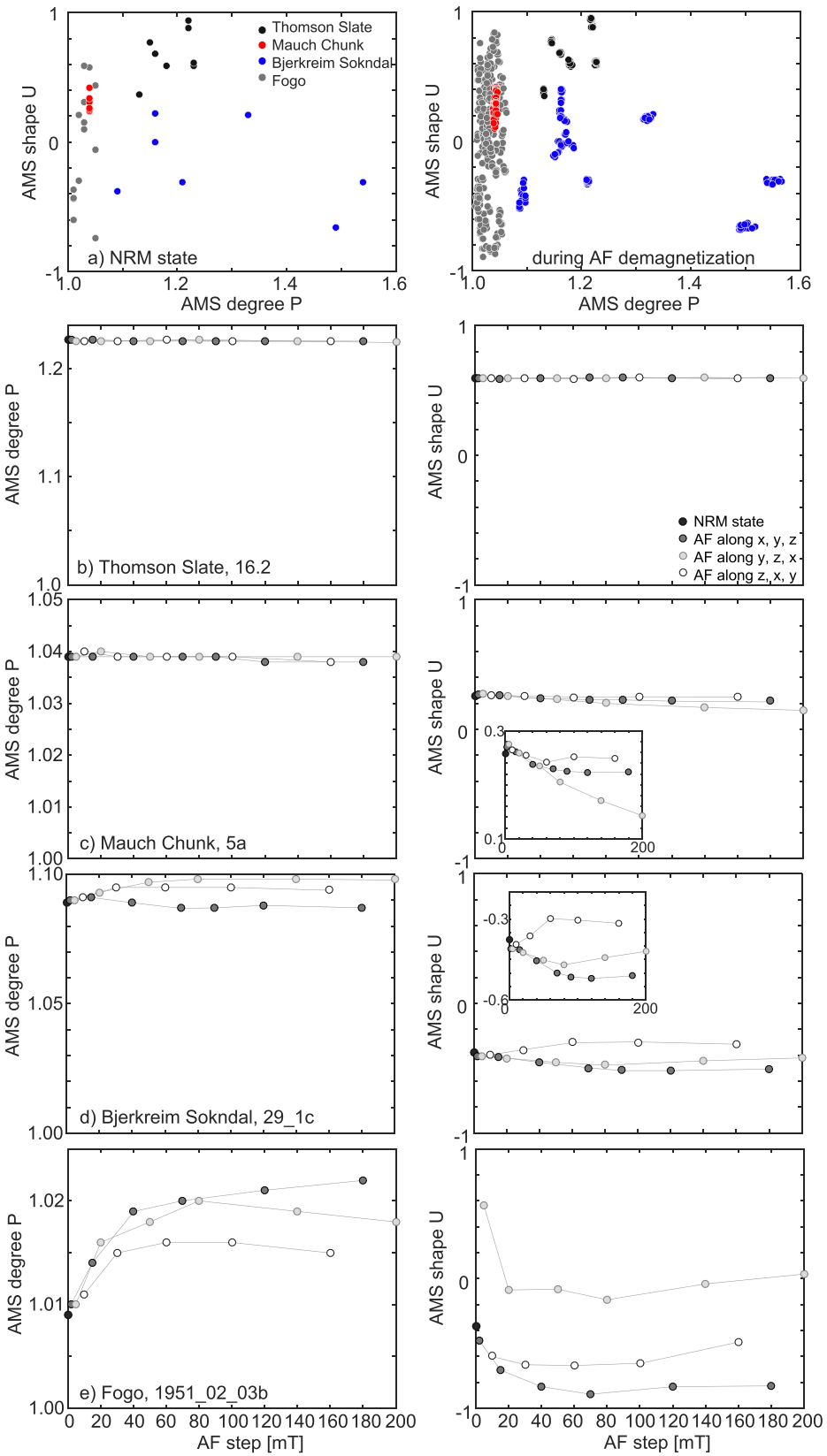


**Figure 2.** (a) P and U in NRM state compared to P and U during AF treatment. (b–e) Variations in P and U with increasing AF field, and order of AF directions, for one representative sample from each lithology. When present, the insets show an expanded view of the U parameter during the entire demagnetization sequence.

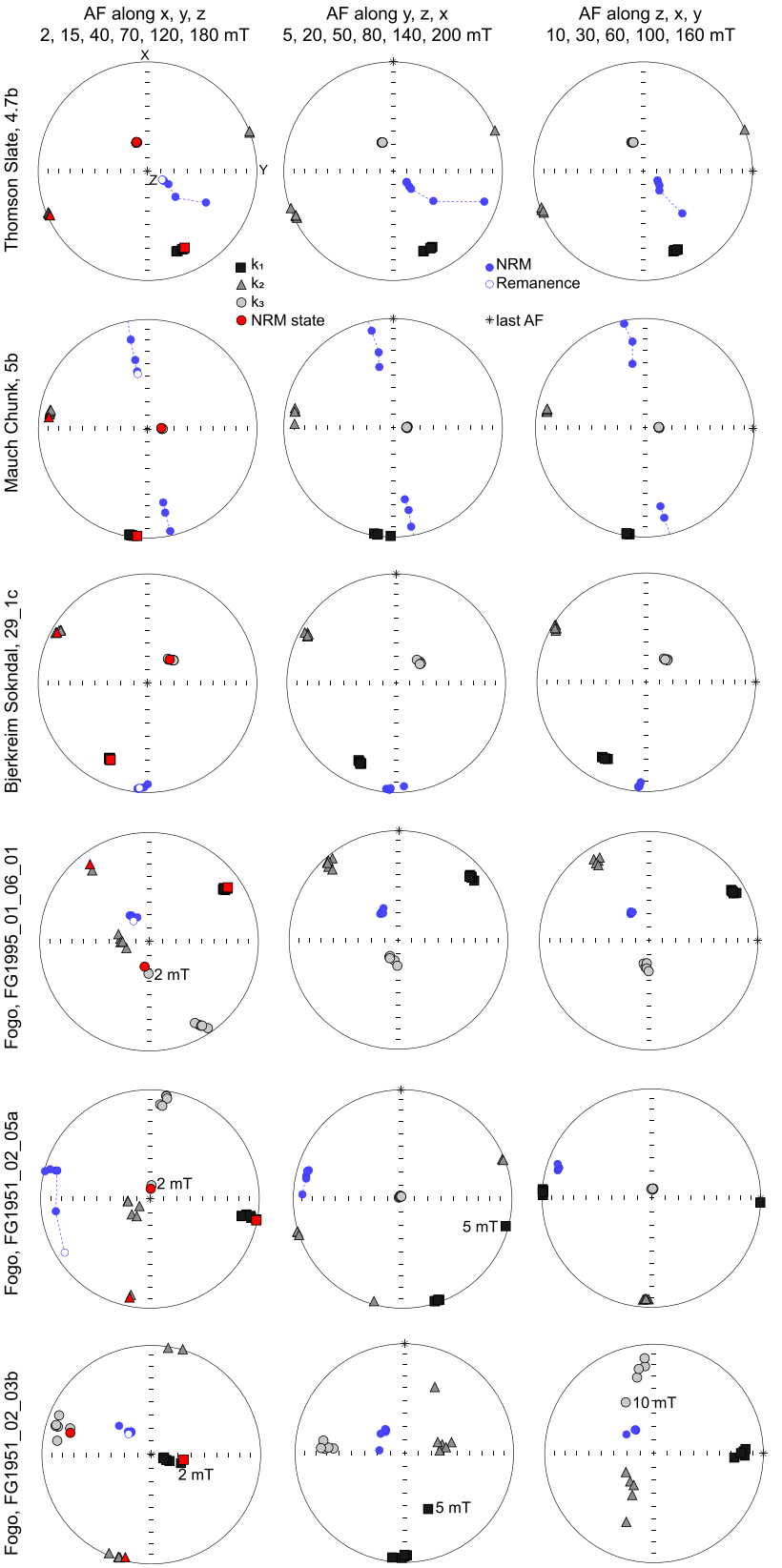


**Figure 3.** Principal AMS directions during AF demagnetization in relation to the remanence direction and last applied AF axis. All remanence directions are plotted on the lower hemisphere. For low AF fields, the AMS axes show intermediate orientations between the NRM state and field-induced anisotropy in higher fields, and these data sets are marked with the corresponding AF value.

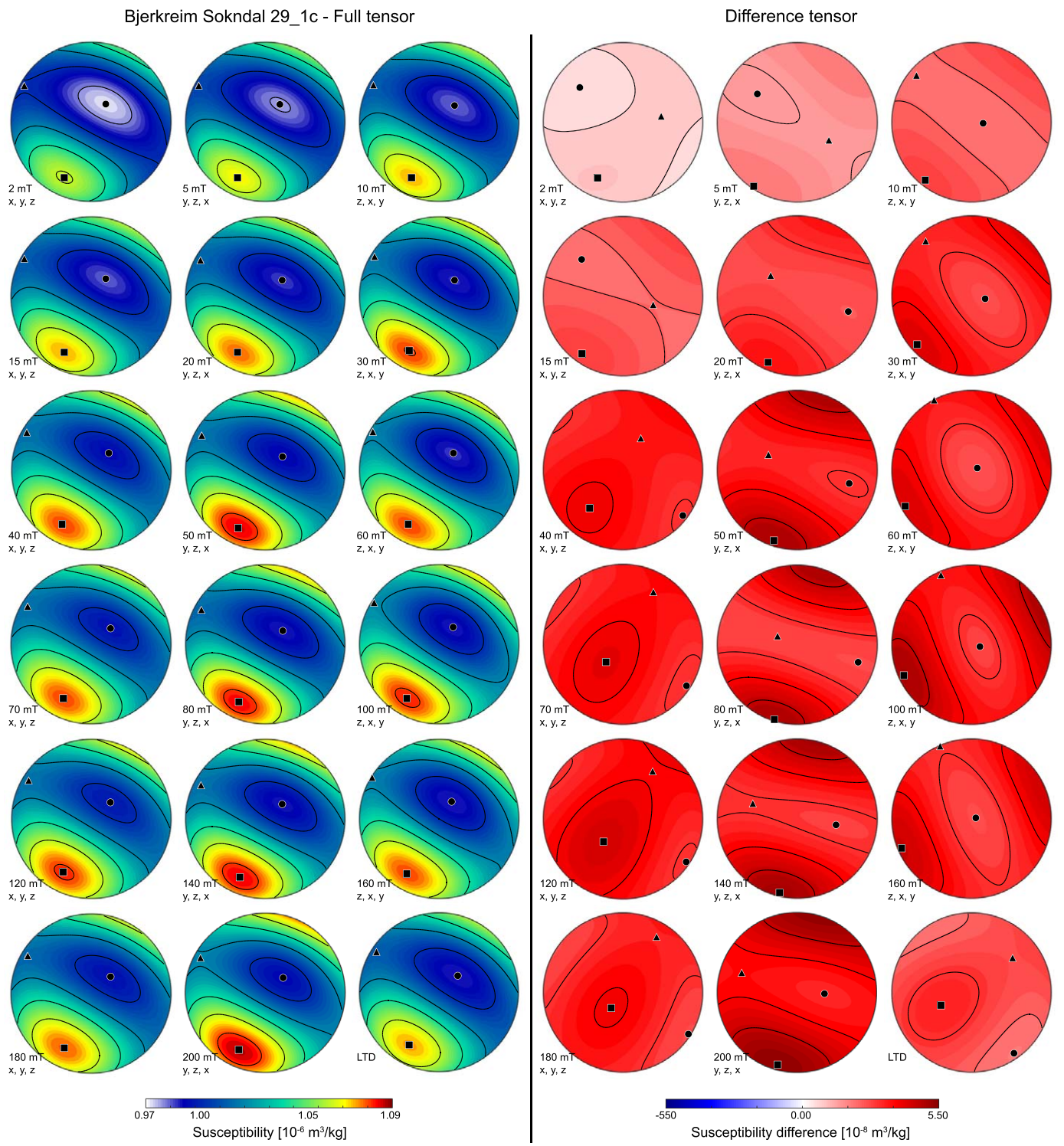


**Figure 4.** Full susceptibility tensors and difference tensors for each demagnetization step during AF and LTD treatments for Bjerkreim Sokndal sample 29_1c. Colorscales indicate the susceptibility magnitude along each direction, projected onto a lower-hemisphere stereoplot. If the susceptibility is represented by a magnitude ellipsoid, one can think of the colors as mapping the ellipsoid radii onto a unit sphere. Contours have a spacing of 0.02 $\times$ $10^{-6}$ $m^3$/kg, and 0.5 $\times$ $10^{-8}$ $m^3$/kg for full and difference tensors, respectively. The most visible effect is the increase in $k_{mean}$ with increasing AF. Even though changes in principal directions are minor, the difference tensors show a clear dependence on the last applied AF direction, particularly for fields >20 mT.

The development of the principal susceptibility directions, and full susceptibility tensor as well as the difference tensors for two samples is shown in Figures 3–5 (and supporting information, Figure S1 and Table S1). Small variations occur for the full tensors of the Thomson Slate, Mauch Chunk formation, and samples from

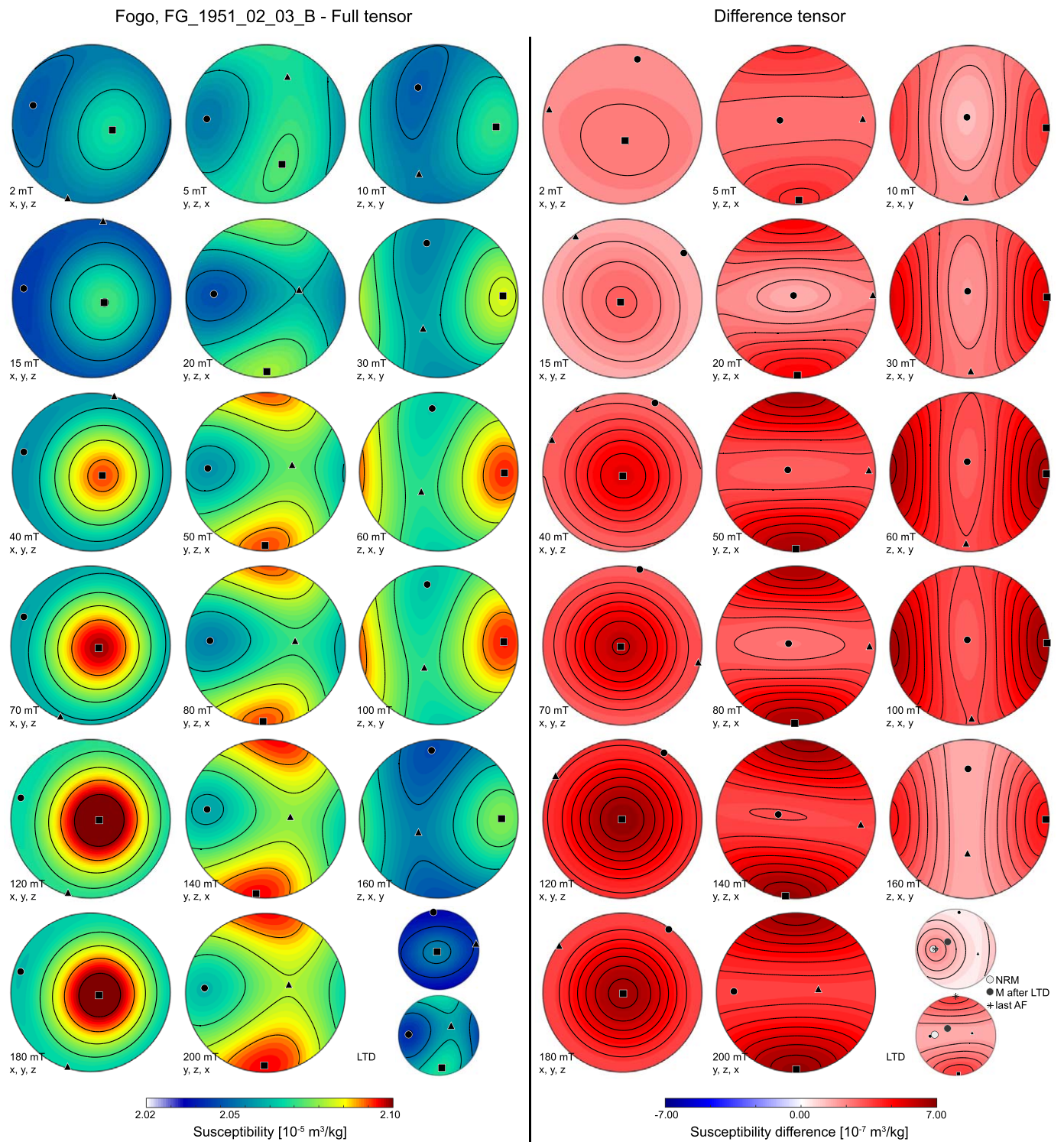


**Figure 5.** Full susceptibility tensors and difference tensors for each demagnetization step during AF and LTD treatments for Fogo basalt FG1951_02_03b. Contours have a spacing of $0.01 \times 10^{-5}$ $m^3/kg$, and $0.5 \times 10^{-7}$ $m^3/kg$ for full and difference tensors, respectively. Both the principal directions of the full tensor, as well as the difference tensors strongly depend on the last applied AF direction. The two LTD experiments show that the effect of the last AF is stronger than the influence of the NRM.

Bjerkreim Sokndal. In particular, the orientation of the principal susceptibility axes remains unchanged (within 95% confidence) during AF treatment to 200 mT. However, difference tensors show a systematic effect of the AF on the AMS, with similar difference tensors in all steps that had the same order of applied

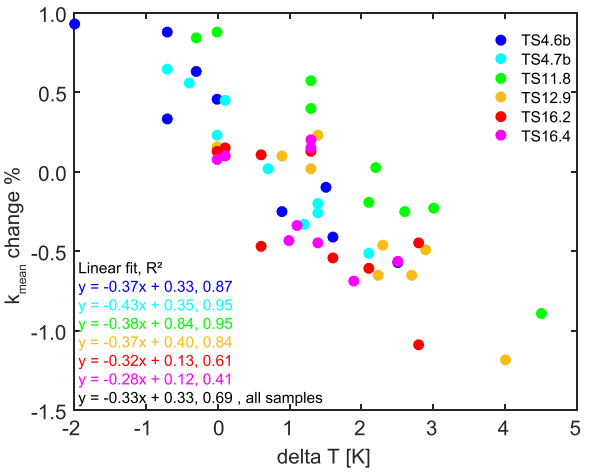


**Figure 6.** Negative correlation between kmean and sample temperature right before AMS measurement.

AF axes, especially in Bjerkreim Sokndal samples. Like for *P* and *U*, the most significant changes are observed in Fogo basalts. Based on the effect of AF treatment on principal susceptibility directions, the basalt samples can be separated into two groups: in the first group, the full tensors and principal axes directions are dominated by the field-imposed anisotropy. In these samples, the $k_1$ axis is consistently aligned with the last applied field direction, and realigns each time the order of AF axes is changed. In other words, the same sample direction can be associated with the maximum, intermediate, or minimum susceptibility, depending on the last applied AF direction. For the second group, principal axes directions also change during AF treatment, however, the effect is smaller, and the axes do not switch completely. For both groups, the difference tensors systematically show a maximum imposed susceptibility parallel to the last applied AF field.

### 3.3. Differences in AMS Tensor Between NRM State and LTD State

For Thomson Slate, Bjerkreim Sokndal, and most Mauch Chunk samples, only minor changes in AMS principal directions are observed between the NRM and LTD states. Two Mauch Chunk samples show a slight rotation of principal axes. The variation in P and U during LTD is generally smaller than during AF demagnetization. Seemingly larger changes in principal directions are observed for the Fogo basalts, however, the AMS observed in these samples after LTD is strongly influenced by the last AF direction that was applied prior to LTD. An additional test involved demagnetizing a sample at low temperature after it had been given an ARM//–*yz* in a 180 mT field, and then demagnetized to 200 mT, with the last AF axis either //*x* (i.e., normal to the ARM) or //–*yz* (i.e., parallel to the ARM). The remaining remanence after AF and LTD demagnetization remained close to the –*yz* axis along which the ARM had been applied. However, the AMS as measured in LTD state reflects the same pattern as that after AF demagnetization: a maximum susceptibility increase was observed parallel to the direction of the last applied AF prior to LTD (supporting information, Figure S2).

## 4. Discussion

### 4.1. Changes in Mean Susceptibility

Increases in mean susceptibility due to AF treatment have been reported previously. For example, *Park et al.* [1988] report 2–25% or 2–7% changes in $k_{mean}$ for the least deformed and most deformed samples in an olivine diabase dyke. *Jordanova et al.* [2007] investigated loess, paleosol, diorite, granite, and gneiss, and found $k_{mean}$ increases between 2 and 27%. Basaltic lava flows from the Deccan Traps, India, display a 8.6% or 5.0% increase in $k_{mean}$ after static and tumbling AF demagnetization, respectively [*Schöbel et al.*, 2013]. A five to eightfold increase in mean susceptibility was observed in mafic dykes from the Henties Bay Outjo Dyke swarm, NW Namibia, after tumbling and static AF demagnetization [*Wiegand*, 2016]. The $\leq 5\%$ increase in $k_{mean}$ observed here is thus in agreement with published results. The decreasing mean susceptibility observed for the Thomson Slate and Mauch Chunk samples subjected to AF fields $> 100$ mT can most likely be explained by heating of the sample during AF treatment. Figure 6 shows the percent change in the mean susceptibility as a function of specimen temperature for several of the Thomson slate specimens. For this, the sample temperature as measured immediately before the AMS measurement after AF treatment at high fields was compared to the sample temperature prior to AMS measurements after AF demagnetization at 70 mT. Other than this temperature effect, changes in mean susceptibility are likely due to changes in wall mobility. For example, if AF demagnetization leads to wall unpinning, the mean susceptibility increases. On the other hand, if the AF-induced domain wall alignment leads to a more stable configuration of domain walls, the susceptibility will decrease.

### 4.2. Changes in AMS During AF Demagnetization and Low-Temperature Demagnetization

The Thomson Slate samples display no systematic change in AMS principal directions or the AMS parameters *P* and *U* during either AF or low temperature demagnetization. Because the AMS of these samples is dominated by paramagnetic minerals [*Johns et al*., 1992; *Kelso et al*., 2002], it is likely that the small amount of ferromagnetic mineral present is not sufficient to have an effect on the AMS, even if domain alignment in magnetite takes place during AF treatment.

The AMS degree of Mauch Chunk red beds remains constant (within error limits) throughout AF treatment to 200 mT. However, the shape of the anisotropy changes, and the changes are strongest when the last applied field was parallel to the sample *x* axis, which is subparallel to the $k_1$ direction. In this case, the AMS shape becomes progressively less oblate with increasing AF fields. While the shape remains oblate for all AF steps, it appears that the magnetic lineation is strengthened when the last AF direction is close to $k_1$. Low-temperature demagnetization can either increase or decrease the *U*-value, and the difference from the shape parameter in the NRM state is generally smaller than the maximum difference observed during AF treatment. AF demagnetization of NRM shows that although most of the NRM is carried by hematite, small amounts of magnetite are present. Most studies attributed field-induced anisotropy to MD magnetite grains [*Potter and Stephenson*, 1990; *Schöbel et al*., 2013; *Violat and Daly*, 1971], and it has also been described in SD maghemite ($\gamma$-$Fe_2O_3$) [*Potter and Stephenson*, 1988]. At present, no studies have investigated whether AF-induced anisotropy occurs in hematite ($\alpha$-$Fe_2O_3$). Therefore, the changes in AMS shape displayed by the Mauch Chunk samples could be attributed to the small amount of magnetite present, but possible contributions from hematite cannot be ruled out.

In the igneous samples from Bjerkreim Sokndal and Fogo, both *P* and *U* are affected by AF treatment as well as low temperature demagnetization. The maximum principal axis of the difference tensors in the Fogo basalts is consistently aligned subparallel to the direction of the last AF axis. The difference tensors for the Bjerkreim Sokndal samples show a similar trend; however, the orientation of the initial AMS fabric also influences their principal axes' orientations. An increase of the susceptibility parallel to the last applied field direction has previously been reported for MD magnetite [*Bhathal and Stacey*, 1969; *Potter and Stephenson*, 1990; *Violat and Daly*, 1971]. Anisotropy degrees of the Bjerkreim Sokndal samples ($P = 1.09 - 1.57$) are consistently higher than those of the Fogo basalts ($P = 1.01 - 1.06$). This may explain why the effect of field-induced anisotropy in the basalts is stronger, because (1) domain realignment will require more energy in grains with elongated shapes and strong SPO than in more equidimensional grains, and (2) a small change in domain alignment will affect a large initial anisotropy less than a small initial anisotropy. Another possible explanation involves the amount and grain size of magnetite. In six samples from Fogo, the field-induced component of the anisotropy has such a strong effect that the principal directions of the full tensor align with $k_1$ subparallel to the last applied field direction. This effect is observed for AF fields as low as 5 mT, in accordance with results shown by *Bhathal and Stacey* [1969], who report effects of field-induced anisotropy in fields of 50 Oersted (5 mT). These changes in AMS principal directions are potentially problematic for lava flow studies, which often rely on the orientation of $k_1$ [e.g., *Cañón-Tapia*, 2004, and references therein]. Changes in principal AMS directions as well as scalar AMS parameters related to AF treatment were also found in lava flows from the Deccan Traps [*Schöbel and de Wall*, 2014], and in 26 out of 48 samples from the Henties Bay Outjo Dyke swarm [*Wiegand*, 2016], interpreted there as an interaction between AMS and NRM.

Low-temperature demagnetization appears to be unable to fully remove the effects of a previous AF-impressed anisotropy. This observation is consistent with findings by *Smirnov et al*. [2017], who state that LTD can be inefficient if grains are oxidized, or due to pinning of walls at exsolution boundaries or lattice defects.

Strong NRMs have been interpreted as affecting AMS in basalts, and therefore it has been suggested to always AF demagnetize such samples prior to measuring AMS [*Schöbel and de Wall*, 2014; *Schöbel et al*., 2013]. The results presented here show clearly that AF demagnetization has the potential to introduce an artificial AMS component, especially in basalts, and should thus be used with caution. This field-imposed anisotropy could not be removed by subsequent low temperature demagnetization. Note that previous studies [*Schöbel and de Wall*, 2014; *Schöbel et al*., 2013] performed AF treatment on tumbling specimens, so that the results are not directly comparable. In this form of AF demagnetization, the sample simultaneously rotates about several axes, resulting in a semirandom rotation, as the AF is applied. This is different from

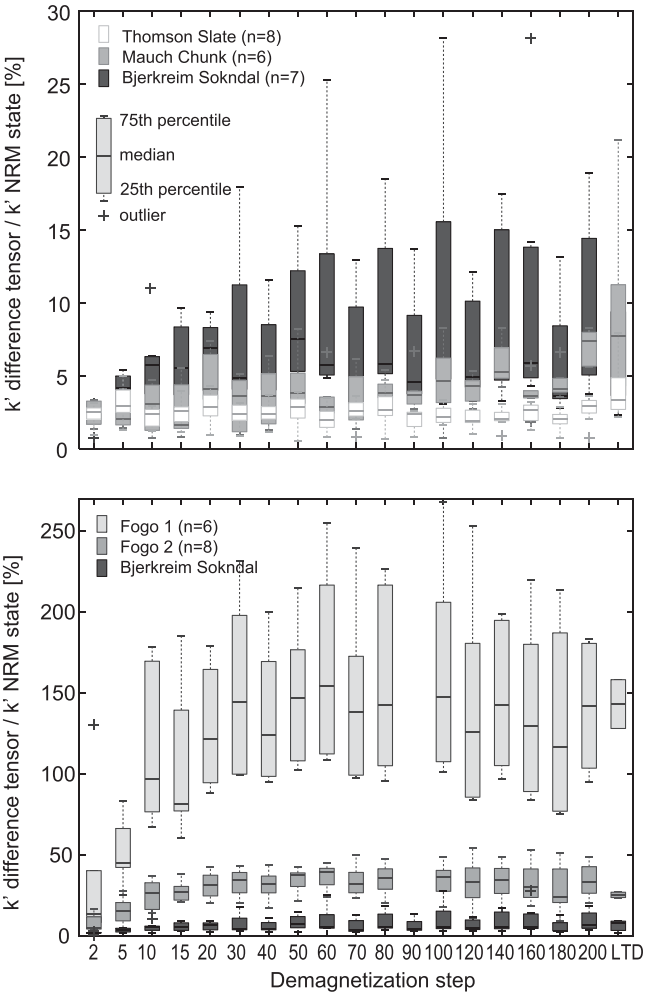


**Figure 7.** Anisotropy degree k' of the difference tensor in comparison to the k' of the sample in NRM state for (top) Thomson Slate, Mauch Chunk, and Bjerkreim Sokndal, and (bottom) Fogo basalts. The Fogo samples were grouped based on k'diff/k'full, where Fogo1 contains samples with k'diff/k'full $>=$ 100% (FG_1951_02_03_B, FG_1951_02_05_A, FG_1951_02_07_A, FG_1951_02_07_C, FG_1951_04_07_C, FG_1951_04_09_C), and Fogo2 samples with k'diff/k'full- $<$ 50% (FG_1951_01_01_B, FG_1995_01_01_02, FG_1995_01_06_01, FG_1995_01_01_05, FG_1995_02_05_C, FG_1995_02_06_B, FG_1995_02_10_C, FG_1995_03_08_A).

the standard static AF demagnetization, during which the AF is subsequently applied to three perpendicular sample directions. *Wiegand* [2016] used three-axis static AF demagnetization for some of their samples, and tumbling AF demagnetization for others. About 22 of their 48 samples showed no or minor effects on the AMS principal directions, and the remaining 26 samples exhibited major changes or switch of principal axes, independent of the type of AF treatment. This can be interpreted as an effect of remanent magnetization, if the change in AMS axes is related to the change in remanence direction, or as a similar field-imposed anisotropy for both the static and tumbling AF demagnetizations.

For any sample with a given coercivity distribution under static AF treatment, all grains experience the same set of antiparallel AF directions when the domain walls lock in. For a tumbling specimen, however, the lock-in AF direction can be different for grains whose coercivities differ. Therefore, any field-imposed anisotropy is expected to be less systematic and weaker in a tumbling AF experiment than what is presented here. This likely explains the weaker change in $k_{mean}$ after tumbling AF demagnetization as opposed to static AF demagnetization described by *Schöbel et al.* [2013]. However, there is no way to control or correct for the field-induced anisotropy in a tumbling AF experiment. Hence, careful investigation and evaluation is needed when interpreting AMS of tumble-AF-demagnetized samples, because it cannot be excluded that field-induced anisotropy contributes significantly to the whole-rock AMS, especially for samples with narrow coercivity distributions. Future studies should systematically investigate the effects of field-induced anisotropy due to tumbling AF demagnetization specifically.

### 4.3. Relative Importance of Field-Induced Anisotropy and Anisotropy Due to CPO or SPO

The influence of field-imposed anisotropy on the overall measured AMS can be negligible (e.g., Thomson Slate samples) to severe, with major changes in principal axes directions, AMS degree and shape (Fogo basalts). In the Mauch Chunk red beds, where the effect of field-induced anisotropy is small, only the shape parameter is affected, whereas the AMS degree and orientation of principal axes appear independent of the applied AF field. A synthetic study investigating the effect of noise on the reliability of AMS data [*Biedermann et al.*, 2013] already demonstrated the higher sensitivity of the AMS shape than other parameters (*P*, principal axes directions) to small changes in directional susceptibilities. For igneous samples from Bjerkreim Sokndal and part of the Fogo basalts, both *U* and *P*, but not the principal directions of the AMS ellipsoid, change due to field-induced anisotropy.

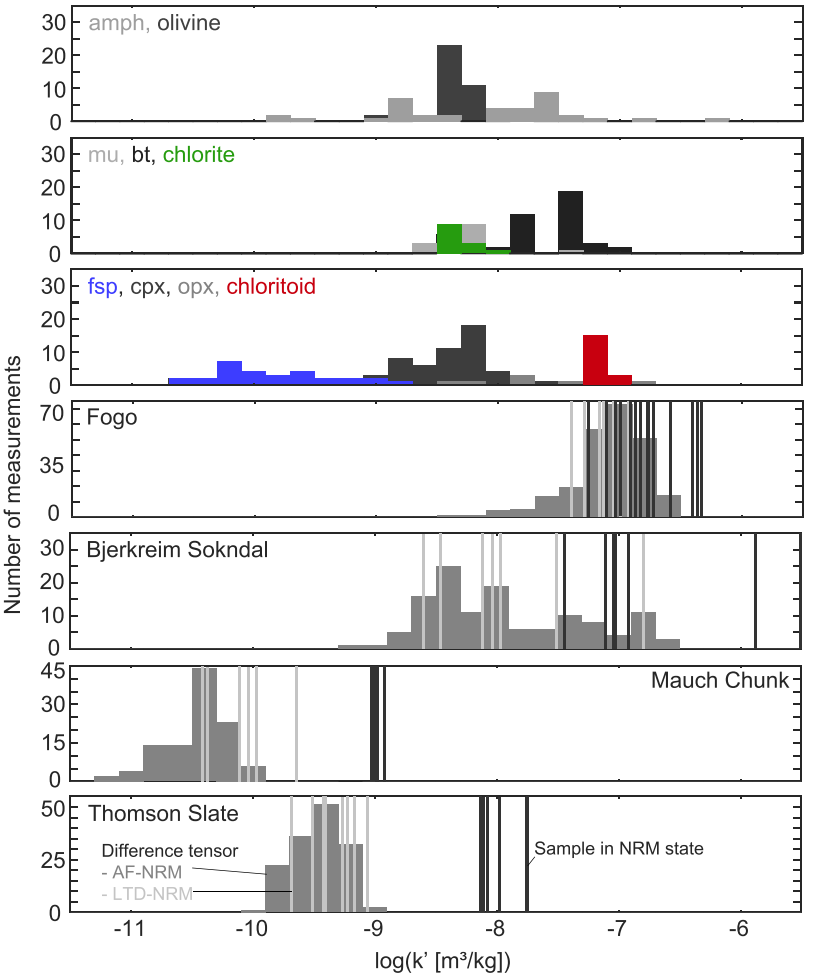


**Figure 8.** Comparison of contributions from field-induced anisotropy to anisotropy in NRM states for all four sample groups, and typical anisotropies of single crystals. Single crystal anisotropies were taken from *Ballet and Coey* [1982], *Beausoleil et al.* [1983], *Belley et al.* [2009], *Biedermann et al.* [2014a, 2014b, 2015a, 2015b, 2016a], *Borradaile et al.* [1987], *Ferré et al.* [2005], *Finke* [1909], *Haerinck et al.* [2013], *Lagroix and Borradaile* [2000], *Martin-Hernandez and Hirt* [2003], and *Wiedenmann et al.* [1986].

The relative contribution of each component of anisotropy depends not only on $P$, but also on the associated mean susceptibility. Therefore, $k' = \mathrm{sqrt}(((k_1 - k_{mean})\text{^}2+(k_2 - k_{mean})\text{^}2+(k_3 - k_{mean})\text{^}2)/3)$ [*Jelinek*, 1984] will be used to investigate the importance of the field-induced AMS relative to the AMS in NRM state. Here, we define the relative importance of field anisotropy as $k'_{diff}/k'_{full}$, i.e., the ratio of field-induced $k'$ (as determined from the difference tensor) and the NRM-state full tensor $k'$. $k'_{diff}/k'_{full}$ is lowest in the Thomson Slate samples, followed by the Mauch Chunk red beds, and Bjerkreim Sokndal igneous rocks. The Fogo basalts are by far the most influenced by field-induced anisotropy, which reaches 270% of the anisotropy in NRM state, i.e., $k'_{diff}/k'_{full} = 2.7$. Additional variation is observed between different Fogo samples, in one group $k'_{diff}/k'_{full}$ is up to 50%, and in the second group it is 100% or more (Figure 7). Principal axes switch for the latter. The importance of field-induced anisotropy as determined from the $k'$ ratio for each sample group is in agreement with the changes in AMS parameters and principal directions. In general, the effect of the field-induced contribution increases with AF field in low fields, consistent with findings by *Violat and Daly* [1971], and then approaches a saturation value. In addition, there appears to be a smaller modification related to the orientation of the last applied AF direction.

Another way to investigate the importance of field-induced anisotropy is to compare the $k'$ of the difference tensors to $k'$ of minerals typically contributing to the CPO-controlled anisotropy, or minerals typically usually making up a large part of a rock. Single crystal $k'$ values are used for this comparison, because they represent the maximum anisotropy a given mineral can cause, when it is perfectly aligned throughout the rock. Given that alignment is never perfect, the anisotropy contribution of these minerals to a rock is likely smaller.

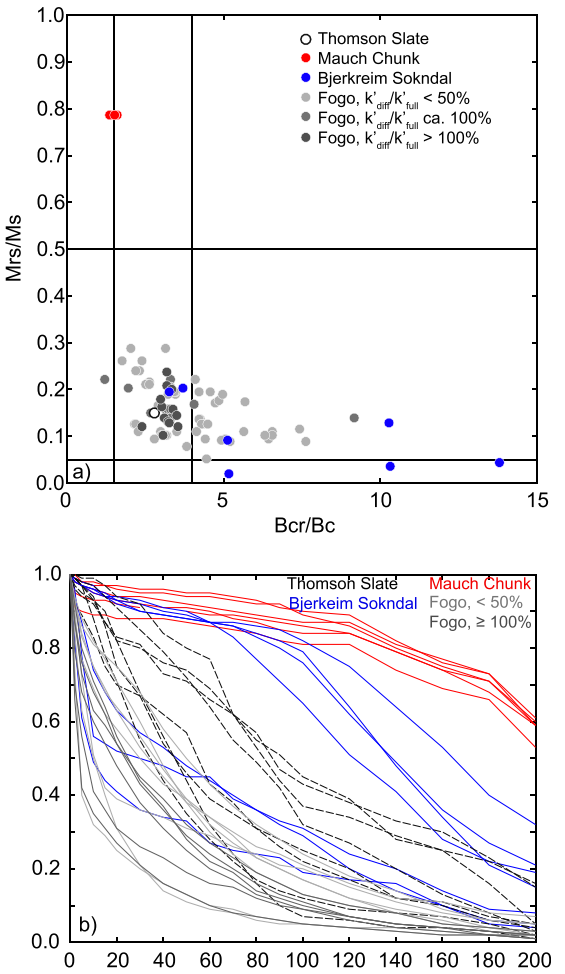


**Figure 9.** (a) Day plot of samples used in this study, and (b) summary of AF demagnetization behaviors.

Figure 8 shows that the anisotropy degree $k'$ of the Mauch Chunk and Thomson Slate field-induced anisotropy is typically less than that of common rock-forming silicates. Thus, the anisotropy of these samples still reflects mineral CPO after AF treatment. However, the field-induced anisotropy of the Fogo basalts is larger than that of most single crystals, thus underscoring the strong influence AF demagnetization has on the anisotropy of these basalts.

Given that field-induced anisotropy can completely dominate the AMS in some samples, e.g., basalt, it would be advantageous to predict which type of samples are prone to strong field-induced effects. *Kapicka* [1981] stated that field-imposed AMS is strongest in rocks with high coercivity. No clear correlation between the $k'_{diff}/k'_{full}$ ratio and either coercivity, remanence coercivity, or *Bcr*/*Bc* was observed in the samples investigated here, however, the strongest field-induced anisotropy is exhibited by samples with $Bc < 20$ mT and $Bcr < 50$ mT. Additionally, Mauch Chunk red beds with highest coercivity show one of the lowest $k'_{diff}/k'_{full}$ ratios. Furthermore, there is no correlation between $k'_{diff}/k'_{full}$ and saturation magnetization (*Ms*) or the ratio of remanence magnetization to saturation magnetization (*Mr*/*Ms*). The Fogo basalts in which field-induced anisotropy outweighs any initial anisotropy plot in the PSD range on a Day plot [*Day et al.*, 1977]. However, Thomson Slate, some Bjerkreim Sokndal samples, and other Fogo samples in which the effect of field-induced anisotropy is smaller, plot in the same field (Figure 9); and there is also no clear correlation to the AF demagnetization behavior. Figure 10 shows the dependence of $k'_{diff}/k'_{full}$ as a function of the initial anisotropy and median destructive field (MDF) of each sample, indicating that the influence of field-induced anisotropy is strongest for samples with *P*-values $<1.1$ and MDFs $< 60$ mT. Therefore, we propose that the relative importance of field-induced anisotropy depends on several factors including (1) contributions of paramagnetic (not affected by field-induced artifacts) and ferromagnetic (in a broad sense; possibly affected by field-induced anisotropy) components to whole-rock anisotropy, (2) the strength of the initial CPO or SPO-based anisotropy (i.e., realignment of domain walls needs more energy for grains with strong shape anisotropy, and the effect will be smaller in comparison), (3) the mineralogy, grain size, oxidation state, and microstructures of grains affected by field-induced anisotropy (stronger effects were observed for MD magnetite as compared to PSD magnetite or hematite; and microstructures affect the grain size), and (4) intensity of applied AF field.

As long as only principal directions, but not AMS degree or shape are of interest, the field-induced contribution to the AMS can likely be neglected in samples whose AMS is dominated by paramagnetic minerals or hematite, and which have a strong initial anisotropy. On the other hand, if AMS is dominated by ferromagnetic minerals (in a broad sense) and the AMS degree is low, it is advisable to check for and quantify effects of field-induced anisotropy.

### 4.4. What is the "True" AMS?

As shown in this study, the same sample can exhibit many different AMS tensors, including changes in AMS shape, degree of anisotropy, and orientation of principal susceptibility directions. In most samples shown here, these differences would not significantly alter a structural interpretation, which is mainly based on the

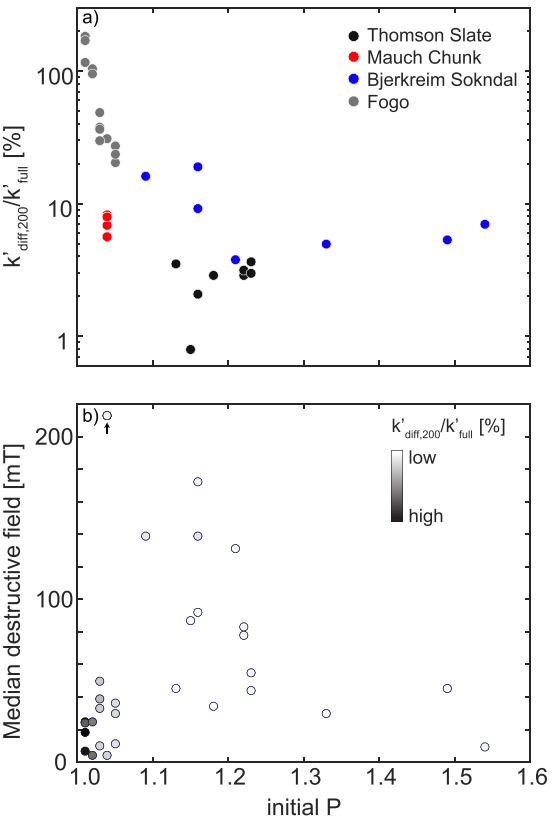


**Figure 10.** (a) Relative importance of field-induced anisotropy as a function of initial anisotropy (i.e., *p*-value in NRM state) and (b) a combination of initial anisotropy and median destructive field.

approximate direction of maximum and minimum principal susceptibility axes. However, for some basalt samples, the orientation of maximum and minimum susceptibility axes change by up to 90°, which would significantly change any structural or flow/emplacement interpretation. If AMS is used as a proxy for mineral fabric, we are interested in (1) magnetocrystalline anisotropy relating to CPO, and (2) shape (self-demagnetization) anisotropy due to SPO of elongated grains. Hence, this AMS tensor should be free of any artifacts, e.g., due to field-induced anisotropy created in the laboratory, due to stress-related pinning of domain walls, or due to NRMs. AF demagnetization may remove pinning sites or NRMs; however, it may also impose an additional AMS component in samples prone to field-induced anisotropy. *Stephenson and Potter* [1996] developed a simple model to quantify the field-induced anisotropy, but more work will be needed before this can be used to correct for these artifacts. Alternatively, high-field methods such as anisotropy determined from hysteresis loops [*Ferré et al.*, 2004; *Kelso et al.*, 2002], torque magnetometry [*Martín-Hernández and Hirt*, 2001, 2004], or anisotropy of isothermal remanent magnetization [*Stephenson et al.*, 1986], for which the sample reaches saturation, should not be affected by either domain wall pinning or by domain realignment. The former two methods have the additional advantage that paramagnetic and ferromagnetic components can be isolated.

## 5. Conclusions

The effects of field-induced anisotropy have been evaluated for 35 samples of different lithologies and initial AMS. AMS shape, degree, and the orientation of principal directions are modified to various extents by the field-induced AMS component. The ratio of field-induced anisotropy to the anisotropy in NRM state ranges from about <2–3% (Thomson Slate) to 270% (Fogo basalt). When this ratio increases, AF treatment affects only *U*, then *U* and *P*, and finally *U*, *P* and the principal susceptibility directions.

The effect of field-induced anisotropy generally increases in low fields before it reaches saturation. Difference tensors show a maximum susceptibility parallel to the last AF axis in samples where the influence of field-imposed anisotropy is strongest. In samples with weaker field-induced anisotropy, or stronger CPO/SPO-based anisotropy, the principal directions of the difference tensors are deviated toward the last AF axis, but still influenced by the initial AMS. The relative importance of field-induced anisotropy depends on the AMS carrier mineral(s), strength of their CPO or SPO, and likely also their oxidation state and microstructures, in addition to the intensity of the applied alternating field. For example, if the AMS is dominated by paramagnetic minerals and hematite with strong CPO, field induced effects can likely be neglected as long as only the principal susceptibility directions are of interest. However, if the main AMS carrier is MD magnetite with weak SPO, field-induced artifacts have to be taken into consideration prior to inferring deformation or flow directions.

Based on the results presented here, we propose that the AMS of samples whose main carriers are ferromagnetic minerals and which have low anisotropy degrees should be checked for field-induced artifacts using the protocols demonstrated here prior to any structural interpretation. High-field methods may be a promising alternative to measure magnetic anisotropy in such samples.

**Acknowledgments**
We are grateful to a number of people who helped collect the samples used in this study. M.J.J. collected the Thomson slate samples with Wei-Wei Sun, with guidance from Peter Hudleston. A.R.B. collected the Bjerkreim Sokndal samples under Swiss National Science Foundation (SNSF) project 155517, together with Alexander Michels, Norwegian University of Science and Technology (NTNU), on fieldwork supported by Research Council of Norway grant 222666 to S.A.M. Fogo basalts were collected under a National Science Foundation (NSF) grant to Brad Singer, and Fogo rock magnetic data was obtained under NSF grant EAR-0911683. This study was funded by the SNSF, project 167608 to A.R.B. Measurements were performed at the Institute for Rock Magnetism (IRM) at the University of Minnesota. The IRM is a US National Multiuser Facility supported through the NSF, Earth Sciences Division, Instrumentation and Facilities program, and by funding from the University of Minnesota. This is IRM publication #1702. The data table can be obtained from the MagIC database, doi:10.7288/V4/MagIC/16232, or the supporting information. We thank editor Thorsten Becker, and reviewers Eric Ferré, Peter Selkin, and an anonymous referee for their constructive comments on the manuscript.

## References

Archanjo, C. J., P. Launeau, and J. L. Bouchez (1995), Magnetic fabric vs. magnetite and biotite shape fabrics of the magnetite-bearing granite pluton of Gameleiras (Northeast Brazil), *Phys. Earth Planet. Inter.*, *89*, 63–75.

Archanjo, C. J., M. G. S. Araujo, and P. Launeau (2002), Fabric of the Rio Ceara-Mirim mafic dike swarm (northeastern Brazil) determined by anisotropy of magnetic susceptibility and image analysis, *J. Geophys. Res.*, *107*(B3), 2046, doi:10.1029/2001JB000268.

Ballet, O., and J. M. D. Coey (1982), Magnetic properties of sheet silicates; 2:1 layer minerals, *Phys. Chem. Miner.*, *8*, 218–229.

Beausoleil, N., P. Lavallee, A. Yelon, O. Ballet, and J. M. D. Coey (1983), Magnetic properties of biotite micas, *J. Appl. Phys.*, *54*, 906.

Belley, F., E. C. Ferre, F. Martin-Hernandez, M. J. Jackson, M. D. Dyar, and E. J. Catlos (2009), The magnetic properties of natural and synthetic $(Fe_xMg_{1-x})_2SiO_4$ olivines, *Earth Planet. Sci. Lett.*, *284*, 516–526.

Bhathal, R. S., and F. D. Stacey (1969), Field-induced anisotropy of magnetic susceptibility in rocks, *Pure Appl. Geophys.*, *76*(1), 123–129.

Biedermann, A. R., W. Lowrie, and A. M. Hirt (2013), A method for improving the measurement of low-field magnetic susceptibility anisotropy in weak samples, *J. Appl. Geophys.*, *88*, 122–130.

Biedermann, A. R., T. Pettke, E. Reusser, and A. M. Hirt (2014a), Anisotropy of magnetic susceptibility in natural olivine single crystals, *Geochem. Geophys. Geosyst.*, *15*, 3051–3065, doi:10.1002/2014GC005386.

Biedermann, A. R., C. Bender Koch, W. E. A. Lorenz, and A. M. Hirt (2014b), Low-temperature magnetic anisotropy in micas and chlorite, *Tectonophysics*, *629*, 63–74.

Biedermann, A. R., T. Pettke, C. Bender Koch, and A. M. Hirt (2015a), Magnetic anisotropy in clinopyroxene and orthopyroxene single crystals, *J. Geophys. Res. Solid Earth*, *120*, 1431–1451, doi:10.1002/2014JB011678.

Biedermann, A. R., C. Bender Koch, T. Pettke, and A. M. Hirt (2015b), Magnetic anisotropy in natural amphibole crystals, *Am. Mineral.*, *100*(8–9), 1940–1951.

Biedermann, A. R., K. Kunze, A. S. Zappone, and A. M. Hirt (2015c), Origin of magnetic fabric in ultramafic rocks, in *IOP Conference Series: Materials Science and Engineering*, vol. 82(1), doi:10.1088/1757-899X/82/1/012098.

Biedermann, A. R., T. Pettke, R. J. Angel, and A. M. Hirt (2016a), Anisotropy of magnetic susceptibility in alkali feldspar and plagioclase, *Geophys. J. Int.*, *205*(1), 479–489.

Biedermann, A. R., F. Heidelbach, M. Jackson, D. Bilardello, and S. A. McEnroe (2016b), Magnetic fabrics in the Bjerkreim Sokndal layered intrusion, Rogaland, southern Norway: Mineral sources and geological significance, *Tectonophysics*, *688*, 101–118.

Bilardello, D., and K. Kodama (2010), A new inclination shallowing correction of the Mauch Chunk Formation of Pennsylvania, based on high-field AIR results: Implications for the Carboniferous North American APW path and Pangea reconstructions, *Earth Planet. Sci. Lett.*, *299*(1–2), 218–227.

Borradaile, G., W. Keeler, C. Alford, and P. Sarvas (1987), Anisotropy of magnetic susceptibility of some metamorphic minerals, *Phys. Earth Planet. Inter.*, *48*, 161–166.

Borradaile, G. J., and B. Henry (1997), Tectonic applications of magnetic susceptibility and its anisotropy, *Earth Sci. Rev.*, *42*, 49–93.

Borradaile, G. J., and M. Jackson (2010), Structural geology, petrofabrics and magnetic fabrics (AMS, AARM, AIRM), *J. Struct. Geol.*, *32*(10), 1519–1551.

Brown, M. C., J. M. Feinberg, and J. A. Bowles (2010), Comparison of palaeointensity methods using historical lavas from Fogo, Cape Verde, Abstract #GP11A-0742 presented at 2010 Fall Meeting, AGU, San Francisco, Calif.

Cañón-Tapia, E. (2004), Anisotropy of magnetic susceptibility of lava flows and dykes: A historical account, in *Magnetic Fabric: Methods and Applications*, edited by F. Martín-Hernández et al., pp. 205–225, Geol. Soc., London, U. K.

Chadima, M., A. Hansen, A. M. Hirt, F. Hrouda, and H. Siemens (2004), Phyllosilicate preferred orientation as a control of magnetic fabric: Evidence from neutron texture goniometry and low and high-field magnetic anisotropy (SE Rhenohercynian Zone of Bohemian Massif), in *Magnetic Fabric: Methods and Applications*, edited by F. Martín-Hernández, et al., pp. 361–380, Geol. Soc., London U. K.

Day, R., M. Fuller, and V. A. Schmidt (1977), Hysteresis properties of titanomagnetites: Grain-size and compositional dependence, *Phys. Earth Planet. Inter.*, *13*, 260–267.

Dunlop, D. J. (2003), Stepwise and continuous low-temperature demagnetization, *Geophys. Res. Lett.*, *30*(11), 1582, doi:10.1029/2003GL017268,

Ferré, E. C., F. Martín-Hernández, C. Teyssier, and M. Jackson (2004), Paramagnetic and ferromagnetic anisotropy of magnetic susceptibility in migmatites: Measurements in high and low fields and kinematic implications. *Geophys. J. Int.*, *157*, 1119–1129.

Ferré, E. C., B. Tikoff, and M. Jackson (2005), The magnetic anisotropy of mantle peridotites: Example from the Twin Sisters dunite, Washington, *Tectonophysics*, *398*, 141–166.

Finke, W. (1909), Magnetische Messungen an Platinmetallen und monoklinen Kristallen, insbesondere der Eisen- Kobalt- und Nickelsalze, *Ann. Phys.*, *336*, 149–168.

Grégoire, V., M. De Saint-Blanquat, A. Nédélec, and J.-L. Bouchez (1995), Shape anisotropy versus magnetic interactions of magnetite grains: Experiments and application to AMS in granitic rocks, *Geophys. Res. Lett.*, *22*(20), 2765–2768.

Grégoire, V., P. Darrozes, P. Gaillot, and A. Nédélec (1998), Magnetite grain shape fabric and distribution anisotropy vs rock magnetic fabric: A three-dimensional case study, *J. Struct. Geol.*, *20*(7), 937–944.

Haerinck, T., T. N. Debacker, and M. Sintubin (2013), Magnetic anisotropy in chloritoid, *J. Geophys. Res. Solid Earth*, *118*, 3886–3898, doi:10.1002/jgrb.50276.

Halgedahl, S., and M. Fuller (1983), The dependence of magnetic domain structure upon magnetization state with emphasis upon nucleation as a mechanism for pseudo-single-domain behavior, *J. Geophys. Res.*, *88*(B8), 6505–6522.

Halgedahl, S. L., and M. Fuller (1981), The dependence of magnetic domain structure upon magnetization state in polycrystalline pyrrhotite, *Phys. Earth Planet. Inter.*, *26*, 93–97.

Henry, B., D. Jordanova, N. Jordanova, J. Hus, J. Bascou, M. Funaki, and D. Dimov (2007), Alternating field-impressed AMS in rocks, *Geophys. J. Int.*, *168*, 533–540.

Hirt, A. M., K. F. Evans, and T. Engelder (1995), Correlation between magnetic anisotropy and fabric for Devonian shales on the Appalachian Plateau, *Tectonophysics*, *247*, 121–132.

Hrouda, F. (1982), Magnetic anisotropy of rocks and its application in geology and geophysics, *Geophys. Surv.*, *5*, 37–82.

Jackson, M., G. J. Borradaile, P. Hudleston, and S. Banerjee (1993), Experimental deformation of synthetic magnetite-bearing calcite sandstones: Effects on remanence, bulk magnetic properties and magnetic anisotropy, *J. Geophys. Res.*, *98*(B1), 383–401.

Jelinek, V. (1977), The Statistical Theory of Measuring Anisotropy of Magnetic Susceptibility of Rocks and its Application, p. 88, Geofyzika Brno, Brno, Czechoslovakia.

Jelinek, V. (1981), Characterization of the magnetic fabric of rocks, *Tectonophysics*, *79*, T63–T67.

Jelinek, V. (1984), On a mixed quadratic invariant of the magnetic susceptibility tensor, *J. Geophys.*, *56*, 58–60.
Jelinek, V. (1996), Measuring Anisotropy of Magnetic Susceptibility on a Slowly Spinning Specimen: Basic Theory, AGICO Print No 10, Brno, Czechoslovakia.
Johns, M. K., M. J. Jackson, and P. J. Hudleston (1992), Compositional control of magnetic anisotropy in the Thomson formation, east-central Minnesota, *Tectonophysics*, *210*, 45–58.
Jordanova, D., N. Jordanova, B. Henry, J. Hus, J. Bascou, M. Funaki, and D. Dimov (2007), Changes in mean magnetic susceptibility and its anisotropy of rock samples as a result of alternating field demagnetization, *Earth Planet. Sci. Lett.*, *255*, 390–401.
Kapicka, A. (1981), Changes of anisotropy of the magnetic susceptibility of rocks induced by a magnetic field, *Stud. Geophys. Geod.*, *25*, 262–274.
Kelso, P. R., B. Tikoff, M. Jackson, and W. Sun (2002), A new method for the separation of paramagnetic and ferromagnetic susceptibility anisotropy using low field and high field methods, *Geophys. J. Int.*, *151*(2), 345–359.
Lagroix, F., and G. J. Borradaile (2000), Magnetic fabric interpretation complicated by inclusions in mafic silicates, *Tectonophysics*, *325*, 207–225.
Lanci, L. (2010), Detection of multi-axial magnetite by remanence effect on anisotropy of magnetic susceptibility, *Geophys. J. Int.*, *181*, 1362–1366.
Liu, Q., Y. Yu, C. Deng, Y. Pan, and R. Zhu (2005), Enhancing weak magnetic fabrics using field-impressed anisotropy: Application to the Chinese loess, *Geophys. J. Int.*, *162*, 381–389.
Lüneburg, C. M., S. A. Lampert, H. D. Lebit, A. M. Hirt, M. Casey, and W. Lowrie (1999), Magnetic anisotropy, rock fabrics and finite strain in deformed sediments of SW Sardinia (Italy), *Tectonophysics*, *307*(1–2), 51–74.
Martín-Hernández, F., and A. M. Hirt (2001), Separation of ferrimagnetic and paramagnetic anisotropies using a high-field torsion magnetometer, *Tectonophysics*, *337*(3–4), 209–221.
Martin-Hernandez, F., and A. M. Hirt (2003), The anisotropy of magnetic susceptibility in biotite, muscovite, and chlorite single crystals, *Tectonophysics*, *367*, 13–28.
Martín-Hernández, F., and A. M. Hirt (2004), A method for the separation of paramagnetic, ferrimagnetic and haematite magnetic subfabrics using high-field torque magnetometry, *Geophys. J. Int.*, *157*(1), 117–127.
Martín-Hernández, F., C. M. Lüneburg, C. Aubourg, and M. Jackson (2004), *Magnetic Fabrics: Methods and Applications*, Geol. Soc., London, U. K.
Martín-Hernández, F., K. Kunze, M. Julivert, and A.M. Hirt (2005), Mathematical simulations of anisotropy of magnetic susceptibility on composite fabrics, *J. Geophys. Res.*, *110*, B06102, doi:10.1029/2004JB003505.
McEnroe, S. A., P. Robinson, and P. T. Panish (2001), Aeromagnetic anomalies, magnetic petrology, and rock magnetism of hemo-ilmenite- and magnetite-rich cumulate rocks from the Sokndal Region, South Rogaland, Norway, *Am. Mineral.*, *86*, 1447–1468.
McEnroe, S. A., L.L. Brown, and P. Robinson (2009), Remanent and induced Magnetic Anomalies over a layered intrusion: Effects from crystal fractionation and recharge events, *Tectonophysics*, *478* 119–134.
Merrill, R. T. (1970), Low-temperature treatments of magnetite and magnetite-bearing rocks, *J. Geophys. Res.*, *75*(17), 3343–3349.
Morris, A., J. S. Gee, N. Pressling, B. E. John, C. J. MacLeod, C. B. Grimes, and R. C. Searle (2009), Footwall rotation in an oceanic core complex quantified using reoriented Integrated Ocean Drilling Program core samples, *Earth Planet. Sci. Lett.*, *287*, 217–228.
Muxworthy, A. R., and E. McClelland (2000), The causes of low-temperature demagnetization of remanence in multidomain magnetite, *Geophys. J. Int.*, *140*, 115–131.
Nagata, T. (1961), *Rock Magnetism*, 2nd ed., Maruzen, Tokyo, Japan.
Nishioka, I., M. Funaki, and T. Sekine (2007), Shock-induced anisotropy of magnetic susceptibility: Impact experiment on basaltic andesite, *Earth Planets Space*, *59*, e45–e48.
Ozima, M., M. Ozima, and S. Akimoto (1964), Low-temperature characteristics of remanent magnetization of magnetite: Self-reversal and recovery phenomena of remanent magnetization, *J. Geomag. Geoelect.*, *16*, 165–177.
Park, J. K., E. I. Tanczyk, and A. Debarats (1988), Magnetic fabric and its significance in the 1400 Ma mealy diabase dykes of Labrador, Canada, *J. Geophys. Res.*, *93*(B11), 13,689–13,704.
Potter, D. K., and A. Stephenson (1988), Field-induced magnetic anisotropy in a dilute dispersion of $\gamma$-$Fe_2O_3$ particles, *J. Appl. Phys.*, *63*(5), 1691–1693.
Potter, D. K., and A. Stephenson (1990), Field-impressed anisotropies of magnetic susceptibility and remanence in minerals, *J. Geophys. Res.*, *95*(B10), 15,573–15,588.
Richter, C., L. Ratschbacher, and W. Frisch (1993), Magnetic fabrics, crystallographic preferred orientation, and strain of progressively metamorphosed pelites in the Helvetic Zone of the Central Alps (Quartenschiefer Formation), *J. Geophys. Res.*, *98*(B6), 9557–9570.
Robinson, P., P. Panish, and S. A. McEnroe (2001), Minor element chemistry of hemo-ilmenite- and magnetite-rich cumulates from the Sokndal Region, South Rogaland, Norway, *Am. Mineral.*, *86*, 1469–1476.
Schmidt, V., A. Hirt, B. Leiss, L. Burlini, and J. Walter (2009), Quantitative correlation of texture and magnetic anisotropy of compacted calcite-muscovite aggregates, *J. Struct. Geol.*, *31*(10), 1062–1073.
Schöbel, S., and H. de Wall (2014), AMS–NRM interferences in the Deccan basalts: Toward an improved understanding of magnetic fabrics in flood basalts, *J. Geophys. Res. Solid Earth*, *119*, 2651–2678, doi:10.1002/2013JB010660.
Schöbel, S., H. de Wall, and C. Rolf (2013), AMS in basalts: Is there a need for prior demagnetization?, *Geophys. J. Int.*, *195*, 1509–1518, doi: 10.1002/2013JB010660.
Siegesmund, S., K. Ullemeyer, and M. Dahms (1995), Control of magnetic rock fabrics by mica preferred orientation - a quantitative approach, *J. Struct. Geol.*, *17*, 1601–1613.
Smirnov, A. V., E. V. Kulakov, M. S. Foucher, and K. E. Bristol (2017), Intrinsic paleointensity bias and the long-term history of the geodynamo, *Sci. Adv.*, *3*, e1602306.
Stacey, F. D. (1961), Theory of the magnetic properties of igneous rocks in alternating fields, *Philos. Mag.*, *6*(70), 1241–1260.
Stacey, F. D. (1963), The physical theory of rock magnetism, *Adv. Phys.*, *12*, 45–133.
Stephenson, A., and D. K. Potter (1996), Towards a quantitative description of field-impressed anisotropy of susceptibility, *Geophys. J. Int.*, *126*, 505–512.
Stephenson, A., S. Sadikun, and D. K. Potter (1986), A theoretical and experimental comparison of the anisotropies of magnetic susceptibility and remanence in rocks and minerals, *Geophys. J. R. Astron. Soc.*, *84*, 185–200.
Stephenson, A., V. Florescu, and N. A. Booth (1995), Field-impressed anisotropy of susceptibility in iron-terbium thin films, *J. Mag. Mag. Mater.*, *145*, 81–84.
Sun, W., P. J. Hudleston, and M. Jackson (1995), Magnetic and petrographic studies in the multiply deformed Thomson Formation, east-central Minnesota, *Tectonophysics*, *249*, 109–124.

Tan, X., and K. Kodama (2002), Magnetic anisotropy and paleomagnetic inclination shallowing in red beds: Evidence from the Mississippian Mauch Chunk Formation, Pennsylvania, *J. Geophys. Res.*, *107*(B11), 2311, doi:10.1029/2001JB001636.

Tarling, D. H., and F. Hrouda (1993), *The Magnetic Anisotropy of Rocks*, Chapman and Hall, London, U. K.

Violat, C., and L. Daly (1971), Anisotropie provoquée sur les roches volcaniques par action d'un champ alternatif, *C. R. hebd. Séances Acad. Sci. Paris Sér. B*, 273, 158–161.

Wiedenmann, A., J.-R. Regnard, G. Fillion, and S. S. Hafner (1986), Magnetic properties and magnetic ordering of the orthopyroxenes FexMg1-xSiO3, *J. Phys. C*, *19*, 3683–3695.

Wiegand, M. (2016), Magmatism and rifting at the South Atlantic margin: Magma transport and emplacement mechanisms of mafic dykes from magnetic studies, PhD thesis, 148 pp., Karlsruhe Inst. of Technol., Karlsruhe, Germany.